B-H Functionalization of Hydrogen-Rich [(Cp*V)(2)(B2H6)(2)]: Synthesis and Structures of [(Cp*V)(2)(B2X2)(2)H-8] (X = CI, SePh; Cp* = eta(5)-C5Me5)

Anagha Haridas, Sourav Kar, Beesam Raghavendra, Thierry Roisnel, Vincent Dorcet, Sundargopal Ghosh

B-H Functionalization of Hydrogen-Rich $[(Cp^*V)_2(B_2H_6)_2]$: Synthesis and Structures of $[(Cp^*V)_2(B_2X_2)_2H_8]$ (X = Cl or SePh; $Cp^* = \eta^5$-C_5Me_5)

Anagha Haridas,[†] Sourav Kar,[†] Beesam Raghavendra,[†] Thierry Roisnel,[‡] Vincent Dorcet,[‡] and Sundargopal Ghosh*,[†]

[†]Department of Chemistry, Indian Institute of Technology Madras, Chennai 600036, India.

[‡]Univ Rennes, CNRS, Institut des Sciences Chimiques de Rennes, UMR 6226, F-35000, Rennes, France.

ABSTRACT: We have recently reported the perchlorinated diniobaborane species $[(Cp^*Nb)_2(B_2H_4Cl_2)_2]$ from $[(Cp^*Nb)_2(B_2H_6)_2]$ using CCl_4 as chlorinating agent. In an attempt to isolate the vanadium analogue, we have isolated $[(Cp^*V)_2(B_2H_6)_2]$, **1** from the reaction of $(Cp^*VCl_2)_3$ with $[LiBH_4{\cdot}THF]$ followed by thermolysis with excess $[BH_3{\cdot}THF]$. Subsequently, the thermolysis of **1** with CCl_4 for a prolonged period of time afforded perchlorinated divanadaborane $[(Cp^*V)_2(B_2H_4Cl_2)_2]$, **2** along with the formation of bichlorinated divanadaborane $[(Cp^*V)_2(B_2H_5Cl)_2]$, **3** and trichlorinated divanadaborane $[(Cp^*V)_2(B_2H_4Cl_2)(B_2H_5Cl)]$, **4**. Similarly, in order to functionalize the terminal B-H by {SePh} group, thermolysis of **1** was carried out with Ph_2Se_2 that yielded persubstituted divanadaborane $[(Cp^*V)_2\{B_2H_4(SePh)_2\}_2]$, **5** in parallel to the formation of $[(Cp^*V)_2\{B_4H_{11}(SePh)\}]$, **6**. Compound **5** is very fascinating in which all the terminal B-H hydrogens of **1** have been substituted by {SePh} ligands. All the compounds have been characterized by ^1H, ^{11}B, ^{13}C NMR spectroscopy; mass spectrometry; IR spectroscopy and single crystal X-ray analysis. Density functional theory (DFT) and TD-DFT calculations provided further understanding regarding the electronic structures, bonding and electronic transitions of these persubstituted vanadaborane species.

INTRODUCTION

In the expansion of rapidly growing polyhedral metallaborane[1a-d] and metallacarborane[1e-f] chemistry, functionalization of borane, metallaborane and carborane at B-H vertices became of interest because of their growing desirability in material science,[2] catalysis[3] and drug design.[4] However, compared to the widely explored carbon-functionalization[5] in hydrocarbons, the boron-functionalization is relatively unexplored.[6] Despite of the efforts devoted to the development of efficient routes for the functionalization of boranes[7] and carboranes,[8] functionalization of metallaboranes met with little success.[9] The icosahedral carboranes and boranes have been functionalized regularly because of their wide-spread applications as a basic component for Boron Neutron Capture Therapy (BNCT),[4a,10] weakly coordinating anion,[11] photoluminescent material,[12] radio imaging reagent,[13] tunable hybrid nanomolecules[14] etc. Reed and co-workers have shown that the hexahalogenated carboranes $[CB_{11}H_6X_6]^-$ (X = Cl, Br or I) play a significant role in stabilization of the coordinatively unsaturated cationic species, such as, the silylium cation (R_3Si^+),[15] fullerene cation (C_{76}^+),[16] hydronium ion ($H_9O_4^+$),[17] and (tetraphenylporphyrinato)iron(III) ion [Fe-(tpp)$^+$].[18] Beginning with the pioneering contributions by Hawthorne[7a-b,8a] and Grimes,[6,8b-c] followed by Xie,[19] Yan,[19a,20] and others,[21,22] several synthetic methodologies have been established for the derivatization of boranes and carboranes. Recently, Spokoyny and co-workers have shown that perfunctionalization of borane clusters using pentafluroroaryl-terminated linkers yields size-tunable rigid nanomolecules that undergo conjugation with different types of thiols via S_NAr chemistry.[14]

After the successful synthesis of perchlorinated rhenaborane $[(Cp^*Re)_2B_5Cl_5H_2]$,[23] search for new routes for the isolation of perhalogenated metallaboranes became of interest. One of the well-known approaches for the B-H functionalization of boranes or carboranes is the electrophilic substitution followed by cross coupling reactions.[24] Having a series of several open and *closo*-metallaboranes,[25-27] we were interested in isolating perhalogenated compounds. Unfortunately, the above mentioned method was not successful for the generation of these species. Note that, recently we have reported various perhalogenated metalloboranes, albeit in lower yields, using $PtBr_2$, CCl_4, $CHCl_3$, MeI, $BHCl_2{\cdot}SMe_2$ as halogenating agents.[25-27] Very recently, we have isolated perchlorinated $[(Cp^*Nb)_2(B_2H_4Cl_2)_2]$ using CCl_4 as chlorine source.[27] As a result, perchlorination of other group 5 metallaboranes became of interest. Herein, in this report, we illustrate the synthesis, structures and bonding of various persubstituted divanadaborane clusters.

RESULTS AND DISCUSSION

Synthesis and reactivity of divanadaborane $[(Cp^*V)_2(B_2H_6)_2]$, 1. Reaction of $[(Cp^*VCl_2)_3]$ with 6 equivalents of $[LiBH_4{\cdot}THF]$ followed by thermolysis with excess $[BH_3{\cdot}THF]$ led to the formation of blue **1** in 31 % yield (Scheme 1). Compound **1** was characterized by mass spectrometric data; ^1H, ^{11}B, ^{13}C NMR spectroscopy and IR spectroscopy. The ^{11}B NMR spectrum showed a resonance at δ = -2.9 ppm. The ^1H NMR spectrum shows the presence of a single Cp* environment. In addition, ^1H NMR spectrum exhibited a chemical shift at -10.12 ppm corresponds to V-*H*-B. Both the ^1H and ^{11}B NMR spectra showed similarity with those of

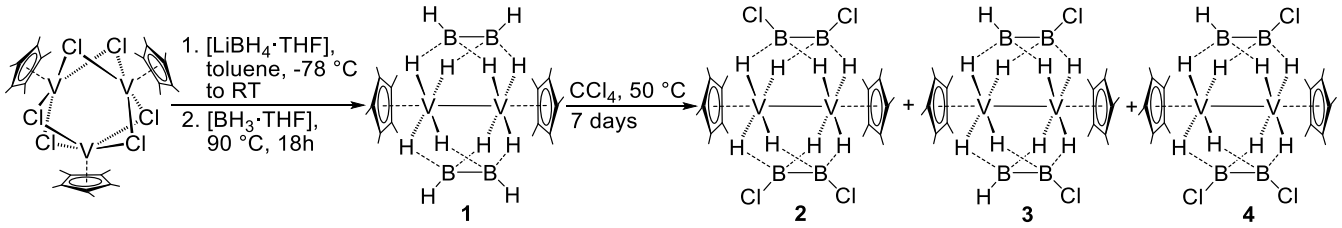

Scheme 1. Synthesis of divanadaborane (1) and chlorinated divanadaboranes (2-4).

$[(CpV)_2(B_2H_6)_2]$.[28] The mass spectrometric data suggests the composition of **1** as $C_{20}H_{42}B_4V_2$.

In order to confirm the spectroscopic assignments of **1**, the single crystal X-ray structure analysis was carried out. As depicted in Figure 1(a), the X-ray analysis revealed compound **1** as the the Cp* analogue of $[(CpV)_2(B_2H_6)_2]$,[28] where two tetrahedral V_2B_2 units are fused by common V-V edge. The V-V, avg. V-B and avg. B-B bond lengths of 2.782, 2.304 and 1.758 Å respectively for **1** are practically analogous to that of $[(CpV)_2(B_2H_6)_2]$.

As shown in Scheme 1, reaction of $[(Cp^*V)_2(B_2H_6)_2]$, **1** with CCl_4 at 50 ˚C for one week led to the formation of violet solid **2**. Room temperature ^{11}B NMR spectrum of **2** reveals a single resonance, appearing at δ = 10.1 ppm. The ^1H NMR spectrum of **2** suggests the presence of one kind of Cp* environment, appeared at δ = 2.18 ppm. In addition, the ^1H NMR spectrum of **2** shows one chemical shift at δ = -8.19 ppm, indicating the existence of V–*H*–B protons. The mass spectrum of **2** exhibited a molecular ion peak at m/z 564.0936 $[M]^+$. The spectroscopic data were not adequate enough to envisage the structure of **2**. The single crystal X-ray analysis was conducted to confirm the structure of **2**.

The X-ray diffraction study exposed the molecular formula of **2** as $[(Cp^*V)_2(B_2H_4Cl_2)_2]$. The solid-state X-ray structure, shown in Figure 1(b), clearly shows that all the terminal B-H hydrogens are functionalized by Cl atoms. The V-V bond distance of **2** (2.8389(6) Å) is slightly longer as compared to **1** (2.7820 (9) Å). Whereas, the average V-B as well as B-B bond distance is comparable with that of **1** (Table 1).

As shown in Scheme 1, in parallel to the formation of per-substituted divanadaborane **2**, the prolonged thermolysis reaction of **1** with CCl_4 also yielded bichlorinated divanadaborane $[(Cp^*V)_2(B_2H_5Cl)_2]$, **3** and trichlorinated divanadaborane $[(Cp^*V)_2(B_2H_4Cl_2)(B_2H_5Cl)]$, **4**. The mass spectra show the molecular ion peaks of **3** and **4** at m/z 496.1801 and 530.1416 for $[M]^+$, suggesting the molecular formula of $C_{20}H_{40}Cl_2V_2B_4$ and $C_{20}H_{39}Cl_3V_2B_4$ respectively. The ^{13}C and ^1H NMR spectra reveals single Cp* environments both for **3** and **4**. The ^{11}B NMR spectrum of **3** displays two boron resonances at δ = 9.0 and -0.5 ppm. The ^1H NMR spectrum of **3** reveals distinct signals at δ = -8.66 and -9.65 ppm in 4:4 ratio for two dissimilar types of bridging V-*H*-B hydrogens. Whereas, the ^{11}B NMR spectrum of **4**, exhibits chemical shifts at δ = 10.3 and -1.6 ppm. The ^1H NMR spectrum of **4** displays peaks at δ = -8.67 and -9.80 ppm in 2:6 ratio that matches to bridging V-*H*-B hydrogens. The IR spectra of **3** and **4** further confirmed the existence of terminal B-H hydrogens. In order to deduce the solid-state X-ray structures of **3** and **4**, the single crystal X-ray analysis was undertaken. The solid state X-ray structure of **3**, shown in Figure S3, is a bichlorinated divanadaborane $[(Cp^*V)_2(B_2H_5Cl)_2]$. Whereas, X-ray analysis of compound **4** showed a trichlorinated divanadaborane $[(Cp^*V)_2(B_4H_9Cl_3)]$ (Figure S4). The V-V bond distances of **3** and **4** are slightly longer as compared to **1**, whereas the avg. B-B and avg.V-B bond lengths are slightly shorter.

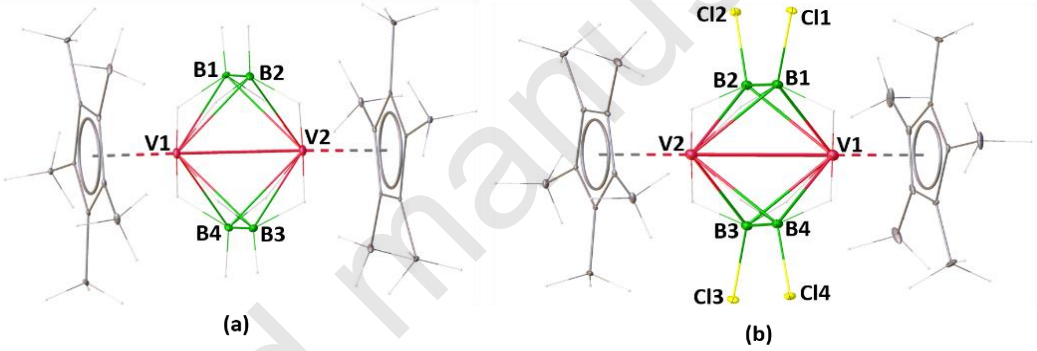

Figure 1. Molecular structures and labeling of **1**(a) and **2**(b). Selected bond lengths [Å] and angles [deg] of **1**: V1-V2 2.7820(9), V1-B1 2.300(4), B2-V1 2.295(4), B3-V1 2.301(4), B4-V1 2.307(4), B1-V2 2.307(4), V2-B2 2.315(4), V2-B3 2.299(4), V2-B4 2.308(4), B1-B2 1.752(7), B3-B4 1.764(6); B2-V1-V2 53.20(11), B2-V1-B1 44.81(16), B2-B1-V1 67.4(2), B2-V1-B1 44.81(16), B1-V1-B4 88.98(16); **2**: V1-V2 2.8389(6), V1-B1 2.302(3), V1-B2 2.302(3), V1-B3 2.306(3), Cl1-B1 1.844(3), Cl2-B2 1.844(3) B2-B1 1.755(5), B3-B4 1.756(5); B2-V1-V2 52.06(8), B1-V2-B2 44.64(12), B2-B1-V1 67.61(16), B2-V1-B1 44.80(12), B1-V1-B4 86.86(12), V1-B2-Cl2 140.52(18),V2-B2-Cl2 143.26(19).

Reactivity of $[(Cp^*V)_2(B_2H_6)_2]$ with Ph_2Se_2. Klumpp and co-workers have introduced R_2S_2 ligands (R = aryl or alkyl) as a source of 'S' and 'SR'.[29] Recently, Himmel and co-workers have synthesized diborane(4) species $[R'SB(\mu\text{-hpp})]_2$ (R' = Bz or Ph) from the reaction of $[HB(\mu\text{-hpp})]_2$ and Bz_2S_2 or Ph_2S_2.[30] We have explored the reactivity of diaryl disulfide, diselenide and ditelluride ligands for the synthesis of various metallaheteroborane clusters. Recently, we have shown that the reaction of divanadaborane $[(CpV)_2(B_2H_6)_2]$ with Bz_2Se_2 or Ph_2S_2 yielded $[(CpV)_2\{B_2H_5(BzSe)\}(B_2H_6)]$, $[(CpV)_2\{B_2H_4(PhS)_2\}\{B_2H_5(PhS)\}]$, and $[(CpV)_2\{B_2H_5(PhS)\}_2]$, albeit in poor yields.[31] In an effort to isolate the persubstituted species, we have carried out the reaction of **1** with Ph_2Se_2 at 90 ˚C. It led to the formation of green solid **5**.

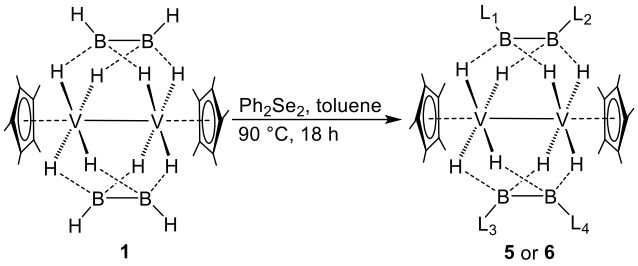

Scheme 2. Synthesis of 5 and 6 (5: L_1 =L_2 = L_3 = L_4 = SePh; 6: L_1 = L_2 = L_3 = H, L_4 = SePh).

The mass spectrum of **5** displays peak at m/z 1048.0567 for $[M]^+$. The ^{1}H NMR spectrum shows single resonance at δ = 1.97 ppm that proposes one kind of Cp* environment. The ^{13}C NMR spectrum further confirms the existence one Cp* environment. The ^{11}B NMR spectrum of **5** shows a single chemical shift at δ = 1.9 ppm. The ^{1}H NMR spectrum of **5** reveals signal for one type of V-*H*-B bridging hydrogens appeared at δ = -7.89 ppm. The IR spectrum of **5** confirmed the presence of V-*H*-B hydrogens. Although all these spectroscopic data suggest a highly symmetric structure of **5**, these data were not enough to predict the structure of **5**. As a result, single crystal X-ray analysis was undertaken on a suitable crystal.

The solid-state X-ray structure of **5**, shown in Figure 2, is $[(Cp^*V)_2\{B_2H_4(SePh)_2\}_2]$, where all the 4 terminal B-H hydrogens are substituted by {SePh} ligand. The V-V bond distance of 2.859 Å is comparatively longer in comparison to its parent divanadaborane **1**. However, the avg. B-B bond distance for **5** (1.741 Å) is slightly shorter to that of **1** and **2**. The avg. B-Se bond distance of **5** (2.033 Å) is analogous to other reported dimetallaselenaborane clusters having B-Se bonds.[31]

As shown in Scheme 2, in parallel to the formation of **5** the thermolysis reaction of **1** with Ph_2Se_2 afforded green solid **6**. The mass spectrum of compound **6** displays molecular ion peak at 584.2027 corresponds to the molecular formula of $C_{26}H_{46}B_4SeV_2$. The ^{1}H and ^{13}C NMR spectra show resonances for one type of Cp* environment. The ^{11}B NMR spectrum of **6** displays two signals at δ = 0.3 and -6.5 ppm. The ^{1}H NMR spectrum shows distinct signals for two different types of bridging V-*H*-B protons at δ = -8.30 and -9.95 ppm. The single crystal X-ray analysis was undertaken to determine the solid-state structure of **6**. The single crystal X-ray study revealed compound **6** as monosubstituted divanadaborane in which one of the terminal B-H hydrogens is substituted by {SePh} ligand. The V-V bond distance of compound **6** is shorter compared to that of per-substituted compound **5**.

As all the divanadaboranes **1-6** have the identical V_2B_4 core, a structural comparison of them became of interest (Table 1). Compounds **1-6** can be viewed as 44 cluster valence electron (cve) species, where two V_2B_2 tetrahedral is fused by one V-V bond. Although, the substituent atoms which form exo-polyhedral bonds with the boron atoms do not affect the skeletal bonding, because of their electronegativity and size difference with boron and hydrogen, they affect the geometrical parameters.[32] On stepwise substitution of hydrogens in **1** by electronegative chlorine atoms, the V-V bond length increases and when all the terminal B-H hydrogens are substituted by Cl atoms, the V-V distance became longer. Likewise, due to the large size of {SePh} ligand, the V-V bond distance increases in **5** and the B-B bond distance decreases upon substitution. On substitution of the hydrogen atoms at B-H in **1** by chlorine, the ^{11}B chemical shifts gradually shifted to down field. However, a minor ^{11}B chemical shift is observed when the substitution was occurred by {SePh} group. These observations may be attributed due to higher electron pulling ability of Cl atoms compared to {SePh} ligands.

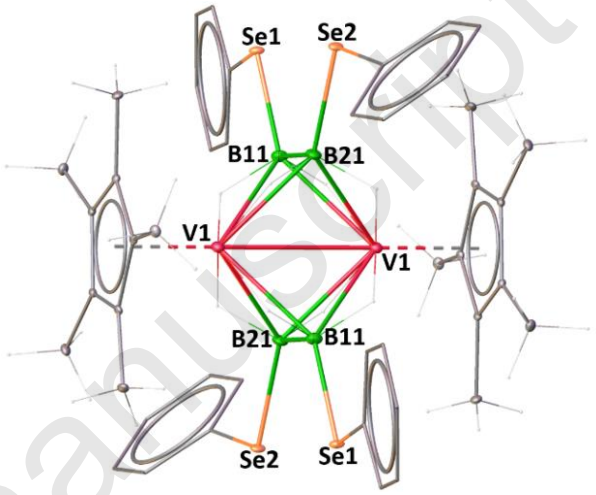

Figure 2. Molecular structure and labeling diagram of **5**. Selected bond lengths [Å] and angles [deg] of **5**: V1-V1 2.8595(10), V1-B11 2.331(3), V1-B21 2.333(3), B11-Se1 2.029(3), B11-B21 1.741(5); V1-V1-B11 52.28(8), B21-V1-B21 104.22(10), B21-V1-B11 87.56(12), B21-V1-B11 44.00(11), V1-B21-V1 75.78(10).

Table 1. Selected structural parameters and spectroscopic data of divanadaboranes.

Av = Average, *d* = distance

Compounds	Av $d_{B\text{-}B}$ [Å]	$d_{V\text{-}V}$ [Å]	δ(V-*H*-B) ^{1}H NMR (ppm)	^{11}B{^{1}H} NMR (ppm)
$[(CpV)_2(B_2H_6)_2]$[28]	1.73	2.787	-9.7	1.7
$[(Cp^*V)_2(B_2H_6)_2]$, **1**	1.758	2.782	-10.12	-2.9
$[(Cp^*V)_2(B_2H_4Cl_2)_2]$, **2**	1.755	2.838	-8.19	10.1
$[(Cp^*V)_2(B_2H_5Cl)_2]$, **3**	1.746	2.794	-8.66, -9.65	9.0, -0.5
$[(Cp^*V)_2(B_2H_4Cl_2)(B_2H_5Cl)]$, **4**	1.740	2.810	-8.67, -9.80	10.3, -1.6
$[(Cp^*V)_2\{B_2H_4(SePh)_2\}_2]$, **5**	1.741	2.859	-7.89	1.9
$[(Cp^*V)_2(B_2H_6)\{B_2H_5(SePh)\}]$, **6**	1.752	2.799	-8.3, -9.95	0.3, -6.5

Electronic structure analysis. To get some insight into the electronic structures and bonding of **1-6**, theoretical calculations on the ground state of DFT at bp86/6-31g* level were carried out. Structural parameters of the optimized structures are almost consistent with the experimental bond lengths (Table S1). The molecular orbital (MO) analysis of **1-4** shows that the HOMOs of these divanadaboranes are centred on both vanadium atoms (d-orbitals). On the other hand, the HOMO of **5** is

localized at the d orbitals of the vanadium centers and the p orbitals of two Se atoms. Likewise, the HOMO of **6** is centred on both vanadium atoms (d-orbital) and one Se atom (p-orbital).

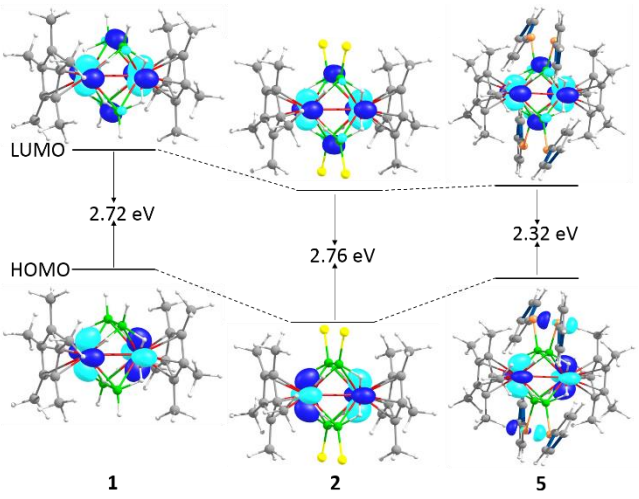

Figure 3. Comparison of frontier molecular orbitals of **1**, **2** and **5**.

Further, the MO analysis of **1**-**6** reveals that the energy gaps between HOMO-LUMO increase in the order of **6** <**5** <**1** < **3** <**4** < **2** (Figure 3 and Table S2). These results have been further confirmed with the calculated natural charges on the vanadium atoms (qV), boron atoms (qB) and substituent atoms (qE) (Table S2). Upon persubstitution by chlorine, the natural charges on boron atoms (qB) become less negative and the natural valence populations around boron atoms decreases. This may be due to the electron pulling effect of chlorine atoms. Thus, the above results satisfyingly support the downfield ^{11}B chemical shifts of the boron atoms attached to chlorine. The HOMO-1 of divanadaboranes **1**-**4** are built of d orbitals of two vanadium atoms which are delocalized over two vanadium centres to form V-V bond. In case of **5**, the HOMO-4 is localised on p orbitals of the Se atoms and d orbitals of two V atoms to form V-V bond. Further, the Laplacian electron density plots for **1**, **2** and **5** show bond critical points (bcp) and bond paths between two vanadium atoms that indicate the presence of V-V bonds (Figure S38 and Table S3).

UV-vis absorption spectra of 1, 2 and 5. In order to investigate the effect on electronic transition upon B-H functionalization by electronegative Cl atoms and {SePh} ligands, UV−vis absorption studies became of interest. The UV−vis absorption studies of **1**, **2** and **5** were performed using CH_2Cl_2 solution. As shown in Figure 4, compound **1** displays absorption peak at λ = 579 nm. The perchlorinated compound **2** shows two absorption peaks at λ = 410 and 565 nm. Whereas, the persubstituted compound **5** shows three absorption bands at λ = 432, 508 and 630 nm. In a comparison of the absorption spectra of **1**, **2** and **5**, a gradual blue shift (**5** < **1** < **2**) has been observed in the region of 650-550 nm.

To confirm these absorptions and get some insight into the electronic transition, we have carried out the time dependent-DFT calculation (Figures 4, S35-S37 and Tables S3-S5). In case of compound **1**, the absorption nearby 579 nm may be assigned to the electronic transition that corresponds to HOMO to LUMO. As HOMO of **1** is centred on d-orbitals of two vanadium and LUMO is localised partially on the d-orbitals of vanadium and B-B bonds, according to TD-DFT calculation the absorption neighbouring 579 nm may be assigned to an intramolecular MLCT transition. The absorption band at 565 nm for **2** corresponds to MLCT, whereas an absorption shoulder near 410 nm seems to be an intramolecular LMCT transition. The intense absorption bands at 630 nm for **5** appears due to the charge transfer from HOMO to LUMO and HOMO-2 to LUMO.

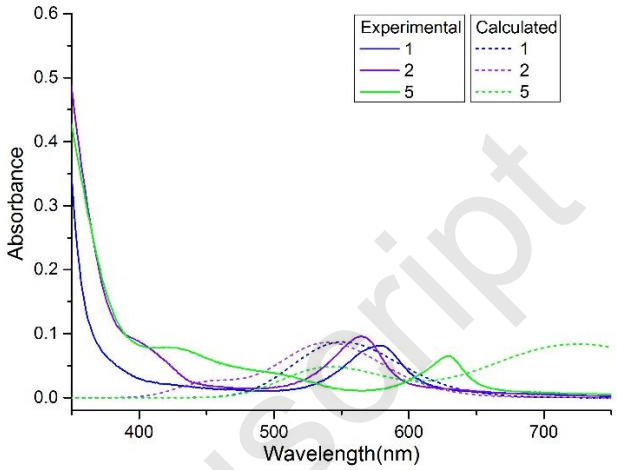

Figure 4. Experimental and calculated UV-vis spectrum of **1**, **2** and **5**.

CONCLUSION

In summary, we have established a very simple and facile method for the perchlorination of $[(Cp^*V)_2(B_2H_6)_2]$, **1** using CCl_4 as chlorine source. Further, we have synthesised persubstituted divanadaborane in which the hydrogens at B-H vertices have been substituted by {SePh} ligands. Upon perchlorination of **1**, the UV-vis absorption spectrum shows a blue shift, while the persubstitution by {SePh} yielded a red shift of the absorption bands.

EXPERIMENTAL SECTION

General procedures and instrumentation. Syntheses of all these compounds were performed underneath of argon pressure using glovebox and Schlenk techniques. Solvents were distilled underneath of N_2 atmosphere using common methods. [$LiBH_4$·THF], [BH_3·THF], CCl_4 and Ph_2Se_2 (Aldrich) were used as purchased. All substances $(Cp^*VCl_2)_3$[33] and $[Bu_4N(B_3H_8)]$[34], reference for $^{11}B\{^1H\}$ NMR spectra were prepared following the literature. On silica-gel TLC plates supported by dialuminium (Merck) thin layer chromatography was carried out. On a Bruker 500 MHz FT-NMR spectrometer all the NMR spectra were recorded. For ^{11}B NMR a sealed tube contains $[Bu_4N(B_3H_8)]$ (δ = −30.07 ppm) in C_6D_6 was taken as an external reference. $^{11}B\{^1H\}$ spectra were processed with a backward linear prediction algorithm to eliminate the broad ^{11}B background signal of the NMR tube.[35] For ^{1}H NMR spectra residual solvent protons were employed as reference (δ = 7.26 ppm, $CDCl_3$; δ = 7.16 ppm, C_6D_6). For $^{13}C\{^1H\}$ NMR spectra residual solvent carbons were employed as a reference (δ = 77.1 ppm, $CDCl_3$; δ = 128.6 ppm, C_6D_6). On a Thermo Scientific (Evolution 300) UV-VIS spectrometer UV-vis absorption spectra were recorded. All the infrared spectra were recorded on a FT/IR-1400 (JASCO) spectrometer. Using 6545 Qtof LC/MS and Qtof Micro YA263 HRMS instruments all the mass spectra were recorded.

Synthesis of 1. In an air and moisture free Schlenk tube, $(Cp^*VCl_2)_3$ (0.50 g, 0.65 mmol) was dissolved in toluene (25 ml) and chilled to -78 ˚C. To the reaction mixture [$LiBH_4$·THF] (1.95 ml, 3.90 mmol) was added slowly using a syringe, and slowly brought to room temperature by stirring for 1 h. Using a syringe BH_3·THF (3.9 ml, 3.90 mmol) was

added, followed by heating at 90 ˚C for 18 h. After evaporation of the solvents under vacuum, it was extracted using hexane/CH_2Cl_2 and celite. After exclusion of the solvent, it was exposed to chromatography on TLC plates and eluted with a CH_2Cl_2/hexane (v/v 30:70) mixture which produced blue [(Cp*V)$_2$B$_4$H$_{12}$] (0.13 g, 31%).

1: MS (ESI$^+$): Calculated for $[C_{20}H_{42}V_2B_4]^+$: 428.2550, found: 428.2530. $^{11}B\{^1H\}$ NMR (160 MHz, 22 °C, $CDCl_3$): δ = -2.9 (4B) ppm. ^1H NMR (500 MHz, 22 °C, $CDCl_3$): δ = 2.06 (s, 30H, C_5Me_5), 2.11 (br., 4H, BH_t), -10.12 (s, 8H, V-*H*-B) ppm. $^{13}C\{^1H\}$ NMR (125 MHz, 22 °C, $CDCl_3$): δ = 113.08 (s, C_5Me_5), 13.01 (s, C_5Me_5) ppm. IR (CH_2Cl_2, cm^{-1}): $\bar{\upsilon}$ = 2404.8 (BH_t).

Synthesis of 2-4. Inside a moisture free Schlenk tube, **1** (0.20g, 0.47 mmol) in CCl_4 (25ml) was stirred at 50 ˚C for 7 days. Conversion of **1** to chloro-substituted products were monitored using TLC. After elimination of the solvent, it was exposed to chromatography on TLC plates. Elution using a CH_2Cl_2/hexane (v/v 30:70) mixture afforded violet coloured compounds **2** (0.03g, 11%), **3** (0.04g, 18%) and **4** (0.05g, 20%). Note that, this reaction produced compound **2** as exclusive product in one day time under reflux condition. We have not observed any chlorination at B-H vertices while we record the NMR. However, keeping it in $CDCl_3$ for prolonged time, led to partial chlorination.

2: MS (ESI$^+$): Calculated for $[C_{20}H_{38}B_4Cl_4V_2]^+$: 564.1003, found: 564.0936. $^{11}B\{^1H\}$ NMR (160 MHz, 22 °C, $CDCl_3$): δ = 10.1 (4B) ppm. ^1H NMR (500 MHz, 22 °C, $CDCl_3$): δ = 2.18 (s, 30H, C_5Me_5), -8.19 (s, 8H, B-*H*-V) ppm. $^{13}C\{^1H\}$ NMR (125 MHz, 22 °C, $CDCl_3$): δ = 117.22 (s, C_5Me_5), 12.31 (s, C_5Me_5) ppm.

3: MS (ESI$^+$): Calculated for $[C_{20}H_{40}B_4Cl_2V_2]^+$: 496.1777, found: 496.1801. $^{11}B\{^1H\}$ NMR (160 MHz, 22 °C, $CDCl_3$): δ = 9.0 (2B), -0.5 (2B) ppm. ^1H NMR (500 MHz, 22 °C, $CDCl_3$): δ = 2.11 (s, 30H, C_5Me_5), 2.58 (br., 2H, BH_t), -8.66 (s, 4H, V-*H*-B), -9.65 (s, 4H, B-*H*-V) ppm. $^{13}C\{^1H\}$ NMR (125 MHz, 22 °C, $CDCl_3$): δ = 115.10 (s, C_5Me_5), 12.67 (s, C_5Me_5) ppm. IR (CH_2Cl_2): $\bar{\upsilon}$ = 2433.7 cm^{-1} (B-H_t).

4: MS (ESI$^+$): Calculated for $[C_{20}H_{39}B_4Cl_3V_2]^+$: 530.1390, found: 530.1416. $^{11}B\{^1H\}$ NMR (160 MHz, 22 °C, $CDCl_3$): δ = 10.3 (1B), -1.6 (3B) ppm. ^1H NMR (500 MHz, 22 °C, $CDCl_3$): δ = 2.10 (s, 30H, C_5Me_5), 2.33 (br., 1H, B-H_t), -8.67 (s, 2H, B-*H*-V), -9.80 (s, 6H V-*H*-B) ppm. $^{13}C\{^1H\}$ NMR (125 MHz, 22 °C, $CDCl_3$): δ = 114.25 (s, C_5Me_5), 12.84 (s, C_5Me_5) ppm. IR (CH_2Cl_2): $\bar{\upsilon}$ = 2433.7 cm^{-1} (B-H_t).

Synthesis of 5 and 6. In a moisture free Schlenk tube, **1** (0.30g, 0.70 mmol) was dissolved in toluene (25 ml) followed by stirring with excess of Ph_2Se_2 (0.66g, 2.10 mmol) for 18 hrs at 90 ˚C. Conversion of **1** to substituted products were monitored using TLC. After exclusion of the solvent, on silica gel TLC plates the residue was exposed to chromatography and eluted using a CH_2Cl_2/hexane (v/v 30:70) mixture which afforded green **5** (0.04g, 6%) and green **6** (0.06g, 16%).

5: MS (ESI$^+$): Calculated for $[C_{44}H_{58}B_4Se_4V_2]^+$: 1048.0521, found: 1048.0567. $^{11}B\{^1H\}$ NMR (160 MHz, 22 °C, $CDCl_3$): δ = 1.9 (4B) ppm. ^1H NMR (500 MHz, 22 °C, $CDCl_3$): δ = 7.13-7.20 (C_6H_5), 1.97 (s, 30H, Cp* C_5Me_5), -7.89 (s, 8H, B-*H*-V) ppm. $^{13}C\{^1H\}$ NMR (125 MHz, 22 °C, $CDCl_3$): δ = 137.38, 130.98, 128.76, 124.74 (C_6H_5), 117.44 (s, C_5Me_5), 11.73 (s, C_5Me_5) ppm.

6: MS (ESI$^+$): Calculated for $[C_{26}H_{46}B_4SeV_2]^+$: 584.2039, found: 584.2027. $^{11}B\{^1H\}$ NMR (160 MHz, 22 °C, $CDCl_3$): δ = 0.3 (1B), -6.5 (3B) ppm. ^1H NMR (500 MHz, 22 °C, $CDCl_3$): δ = 7.09-7.16 (C_6H_5), 2.16 (s, 30H, C_5Me_5), 2.47 (br, 3H, B-H_t), -8.30 (s, 2H, B-*H*-V), -9.95 (s, 6H, V-*H*-B) ppm. $^{13}C\{^1H\}$ NMR (125 MHz, 22 °C, $CDCl_3$): δ = 138.31, 130.18, 127.66, 123.70 (C_6H_5), 114.30 (s, C_5Me_5), 12.73 (s, C_5Me_5) ppm. IR (CH_2Cl_2): $\bar{\upsilon}$ = 2403.8 cm^{-1} (B-H_t).

X-ray crystal structure determinations. The X-ray crystal data of compounds **1** and **3-6** were collected at 150 K and integrated in a D8 VENTURE Bruker AXS diffractometer under graphite-monochromated MoK$_\alpha$ radiation (λ = 0.71073 Å). Using a Bruker APEX-II CCD diffractometer equipped with graphite-monochromated MoK$_\alpha$ radiation (λ = 0.71073 Å), X-ray crystal data of compound **2** was collected at 296 K and integrated. Using SADABS[36] program multi-scan absorption correction has been done on the X-ray crystal data. All the structures were solved employing SHELXS-97 or SIR92 and refined with SHELXL-2014.[37] Using Olex2[38] all the molecular structures were drawn. CCDC 1940467 (**1**), 1940465 (**2**), 1940441(**3**), 1940442(**4**), 1940439(**5**) and 1940466 (**6**) contains crystallographic data. These data are available free of charge at www.ccdc.cam.ac.uk/data_request/cif.

Crystal data of 1. $C_{20}H_{42}B_4V_2$, *Mr* = 427.65 g.mol^{-1}, Monoclinic, *P*21/n, *a* = 11.3343(9) Å, *b* = 14.6762(10) Å, *c* = 14.5522(10) Å, α = 90°, β = 109.887(2)°, γ = 90°, *V* = 2276.3(3) Å^3, ρ_{calcd} = 1.248 g.cm^{-3}, *Z* = 4, μ = 0.823 mm^{-1}, *F*(000) = 912, GOF = 1.061, R_1 = 0.0866, wR_2 = 0.2490, reflections collected 18801, independent reflections 5086 ($2\theta \leq 54.954°$) and 281 parameters.

Crystal data of 2. $C_{20}H_{38}B_4Cl_4V_2$, *Mr* = 565.42 g.mol^{-1}, Monoclinic, *P*21/n, *a* = 10.4129(4)Å, *b* = 17.7675(7)Å, *c* =14.8537(5) Å, α = 90°, β = 98.7410(18)°, γ = 90°, *V* = 2716.18(18) Å^3, ρ_{calcd} = 1.383 g.cm^{-3}, *Z* = 4, μ = 1.089 mm^{-1}, *F*(000) = 1560, GOF = 1.028, R_1 = 0.0389, wR_2 = 0.1075, reflections collected 21357, independent reflections 4784 ($2\theta \leq 49.992°$) and 313 parameters.

Crystal data of 3. $C_{20}H_{40}B_4Cl_2V_2$, *Mr* = 496.18 g.mol^{-1}, Orthorhombic, *Pnma*, *a* = 20.5180(11) Å, *b* = 15.4472(9) Å, *c* =7.6522(4) Å, α = β = γ = 90°, *V* = 2425.3(2) Å^3, ρ_{calcd} = 1.266 g.cm^{-3}, *Z* = 4, , μ = 0.884 mm^{-1}, *F*(000) = 976, GOF = 1.186, R_1 = 0.0441, wR_2 = 0.0983, reflections collected 17157, independent reflections 2862 ($2\theta \leq 54.963°$) and 160 parameters.

Crystal data of 4. $C_{20}H_{31}B_4Cl_3V_2$, *Mr* = 522.92 g.mol^{-1}, monoclinic, *P*21, *a* = 7.9109(6) Å, *b* = 15.3964(9) Å, *c* = 10.8018(7) Å, α = γ = 90°, β = 101.498(3)°, *V* = 1289.25(15) Å^3, ρ_{calcd} = 1.347 g.cm^{-3}, *Z* = 2, μ = 1.041 mm^{-1}, *F*(000) = 536, GOF = 1.080, R_1 = 0.1035, wR_2 = 0.2840, reflections collected 9083, independent reflections 5318 ($2\theta \leq 54.964°$) and 150 parameters.

Crystal data of 5. $C_{44}H_{58}B_4Se_4V_2$, *Mr* = 1047.86 g.mol^{-1}, Triclinic, *P*-1, *a* = 10.6356(14) Å, *b* = 10.7180(13) Å, *c* = 11.2446(15) Å, α = 106.352(4) °, β = 113.721(4)°, γ = 96.642(4)°, *V* = 1087.1(2) Å^3, ρ_{calcd} = 1.601 g.cm^{-3}, *Z* = 1, μ = 3.809 mm^{-1}, *F*(000) = 524, GOF = 1.052, R_1 = 0.0441, wR_2 = 0.1273, reflections collected 21602, independent reflections 4991 ($2\theta \leq 55.102°$) and 261 parameters.

Crystal data of 6. $C_{26}H_{46}B_4SeV_2$, *Mr* = 582.71 g.mol^{-1}, Triclinic, *P*-1, *a* = 8.1846(6) Å, *b* = 10.2047(7) Å, *c* = 18.8337(14) Å, α = 105.551(2)°, β = 92.550(3)°, γ = 107.010(3)°, *V* = 1436.18(18) Å^3, ρ_{calcd} = 1.347 g.cm^{-3}, *Z* = 2, μ = 1.931 mm^{-1}, *F*(000) = 604, GOF = 1.029, R_1 = 0.0290, wR_2 = 0.0717, reflections collected 33324, independent reflections 6577 ($2\theta \leq 54.968°$) and 341 parameters.

Computational Details. Optimization of all the molecules are done using the Gaussian 09[39] program. The gradient-corrected bp86[40] functional along with 6-31g* basis set had been employed for the optimization. Starting from X-ray crystallographic coordinates the model compounds were fully optimized without any solvent effect in gaseous state. Frequency calculations were carried out at the same level of theory. With the natural bond orbital (NBO) partitioning scheme[41] as employed in the Gaussian 09 programs natural bonding analyses were executed. Multiwfn V.3.6 package[42] was used to carry out the QTAIM analysis. All the optimized structures and orbital pictures were created with the Gaussview[43] and Chemcraft[44] programs.

ASSOCIATED CONTENT

Supporting Information

Details of X-ray structures, spectroscopic data, DFT and TD-DFT. The supporting Information is available free of charge on the ACS publication website.

AUTHOR INFORMATION

Corresponding Author

*E-mail: sghosh@iitm.ac.in. Fax: +91 44-22574202. Tel: +91 44-22574230.

Notes

The authors declare no competing financial interests.

ACKNOWLEDGMENT

Generous support from the Council of Scientific and Industrial Research, CSIR (Project No. 01(2939)/18/emr-ii), India, is gratefully acknowledged. A. H. thank CSIR, India; S. K. and B. R. thank IIT Madras respectively for fellowship. We are thankful to Venkatachalam Ramkumar, IIT Madras for X-ray Support. We also gratefully computational center of IIT Madras.

REFERENCES

(1) (a) Fehlner, T. P., Ed. *Inorganometallic Chemistry*; Plenum: New York, 1992. (b) Ghosh, S.; Noll, B. C.; Fehlner, T. P. Borane Mimics of Classic Organometallic Compounds: $[(Cp^*Ru)(B_8H_{14})(RuCp^*)]^{0,+1}$ Isoelectronic Analogues of Dinuclear Pentalene Complexes. *Angew. Chem. Int. Ed.* **2005**, *44*, 6568-6571. (c) Ghosh, S.; Noll, B. C.; Fehlner, T. P. Expansion of iridaborane clusters by addition of monoborane. Novel metallaboranes and mechanistic detail. *Dalton Trans*. **2008**, 371-378. (d) Bose, S. K.; Geetharani, K.; Sahoo, S.; Reddy, K. H. K.; Varghese, B.; Jemmis, E. D.; Ghosh, S. Synthesis, Characterization, and Electronic Structure of New Type of Heterometallic Boride Clusters. *Inorg. Chem.* **2011**, *50*, 9414–9422. (e) Saxena, A. K.; Hosmane, N. S. Recent advances in the chemistry of carborane metal complexes incorporating d- and f-block elements. *Chem. Rev.* **1993**, *93*, 1081-1124. (f) Carr, M. J.; Franken, A.; Macías, R.; Xiedy, J. D. Twelve-vertex polyhedral carbaborane chemistry. Isostructural cations and anions: The 'globule–globule' salt $[H_3NCH_2C_2B_{10}H_{11}]$ $[H_3CCH_2C\text{-}B_{11}H_{11}]$. *Polyhedron* **2006**, *25*, 1069-1075.

(2) (a) Carter, T. J.; Mohtadi, R.; Arthur, T. S.; Mizuno, F.; Zhang, R.; Shirai, S.; Kampf, J. W. Boron clusters as highly stable magnesium-battery electrolytes. *Angew. Chem., Int. Ed.* **2014**, *53*, 3173−3177. (b) Núñez, R.; Romero, I.; Teixidor, F.; Viñas, C. Carboranes as a Tool to Tune Phosphorescence *Chem. Soc. Rev.* **2016**, *45*, 5147−5173.

(3) (a) Hlatky, G. G.; Turner, H. W.; Eckman, R. R. Ionic, base-free zirconocene catalysts for ethylene polymerization. *J. Am. Chem. Soc.* **1989**, *111*, 2728-2729. (b) Hlatky, G. G.; Eckman, R. R.; Turner, H. W. Metallacarboranes as labile anions for ionic zirconocene olefin polymerization catalysts. *Organometallics* **1992**, *11*, 1413-1416.

(4) (a) Soloway, A. H.; Tjarks, W.; Barnum, B. A.; Rong, F. G.; Barth, R. F.; Codogni, I. M.; Wilson, J. G. The Chemistry of Neutron Capture Therapy. *Chem. Rev.* **1998**, *98*, 1515-1562. (b) Sivaev, I. B.; Bregadze, V. V. Polyhedral Boranes for Medical Applications: Current Status and Perspectives. *Eur. J. Inorg. Chem.* **2009**, 1433−1450. (c) Issa, F.; Kassiou, M.; Rendina, L. M. Boron in drug discovery: carboranes as unique pharmacophores in biologically active compounds. *Chem. Rev.* **2011**, *111*, 5701−5722.

(5) (a) Davies, H. M. L.; Morton, D. Recent Advances in C–H Functionalization. *J. Org. Chem.* **2016**, *81*, 343-350. (b) Dick, A. R.; Hull, K. L.; Sanford, M. S. A Highly Selective Catalytic Method for the Oxidative Functionalization of C−H Bonds. *J. Am. Chem. Soc.* **2004**, *126*, 2300-2301.

(6) (a) Stockman, K. E.; Boring, E. A.; Sabat, M.; Finn, M. G.; Grimes, R. N. Small Carborane Ligands as Tailorable Cp Surrogates. Halogenation, Alkylation, and Arylation at Metal and Cage Positions on $CpX_2M(Et_2C_2B_4H_4)$ Complexes (M = Ta, Nb). *Organometallics* **2000**, *19*, 2200-2207. (b) Russell, J. M.; Sabat, M.; Grimes, R. N. Organotransition-Metal Metallacarboranes. 59.[1] Synthesis and Linkage of Boron-Functionalized Ferracarborane Clusters. *Organometallics* **2002**, *21*, 4113-4128. (c) Grimes, R. N. In *Comprehensive Organometallic Chemistry II*; Abel, E. W.; Stone, F. G. A.; Wilkinson, G., Eds.; Pergamon Press: Oxford, England, 1995; *vol. 1*.

(7) (a) Peymann, T.; Knobler, C. B.; Hawthorne, M. F. An Icosahedral Array of Methyl Groups Supported by an Aromatic Borane Scaffold: The $[closo\text{-}B_{12}(CH_3)_{12}]^{2-}$ Ion. *J. Am. Chem. Soc.* **1999**, *121*, 5601-5602. (b) Maderna, A.; Knobler, C. B.; Hawthorne, M. F. Twelvefold functionalization of an icosahedral surface by total esterification of $[B_{12}(OH)_{12}]^{2-}$: 12(12)-closomers. *Angew. Chem. Int. Ed.* **2001**, *40*, 1662-1664. (c) Van, N.; Tiritiris, I.; Winter, R. F.; Sarkar, B.; Singh, P.; Duboc, C.; Mulñoz-Castro, A.; Arratia-Perez, R.; Kaim, W.; Schleid, T. Oxidative Perhydroxylation of $[closo\text{-}B_{12}H_{12}]^{2-}$ to the Stable Inorganic Cluster Redox System $[B_{12}(OH)_{12}]^{2-/-}$: Experiment and Theory. *Chem. Eur. J.* **2010**, *16*, 11242-11245.

(8) (a) Jiang, W.; Knobler, B.; Mortimer, M. D.; Hawthorne, M. F. A Camouflaged Icosahedral Carborane: Dodecamethyl-1,12-dicarba-closo dodecaborane(12) and Related Compounds. *Angew. Chem. Int. Ed.* **1995**, *34*, 1332-1333. (b) Benvenuto, M. A.; Sabat, M.; Grimes, R. N. Organotransition-metal metallacarboranes. 29. Synthesis of selectively C- and B-substituted double- and triple-decker sandwiches. $(\eta^5\text{-}C_5Me_5)Co^{III}(\eta^5\text{-}R_2C_2B_3R'_3H_2)$ cobaltocenium analogs. *Inorg. Chem.* **1992**, *31*, 3904-3909. (c) Yao, H.; Grimes, R. N. Small cobaltacarborane clusters in synthesis. Peralkylation, perhalogenation, and macrocycle construction. *J. Organomet. Chem.* **2003**, *680*, 51-60.

(9) (a) Gilbert, K. B.; Boocock, S. K.; Shore, S. G. Comprehensive Organometallic Chemistry. In *Compounds with Bonds between a Transition Metal and Boron*; Wilkinson, G.; Stone, F. G. A.; Abel; E. W., Eds.; Pergamon: New York, 1982; *vol. 6*, pp 879-945. (b) Bose, S. K.; Geetharani, K.; Ghosh, S. C–H activation of arenes and heteroarenes by early transition metallaborane, $[(Cp^*Ta)_2B_5H_{11}]$ ($Cp^* = \eta^5\text{-}C_5Me_5$). *Chem. Commun.* **2011**, *47*, 11996–11998.

(10) Hawthorne, M. F. The Role of Chemistry in the Development of Boron Neutron Capture Therapy of Cancer. *Angew. Chem. Int. Ed. Engl.* **1993**, *32*, 950-984.

(11) (a) Reed, C. A. Carboranes: A New Class of Weakly Coordinating Anions for Strong Electrophiles, Oxidants, and Superacids. *Acc. Chem. Res.* **1998**, *31*, 133-139. (b) Strauss, S. H. The search for larger and more weakly coordinating anions. *Chem. Rev.* **1993**, *93*, 927.

(12) (a) Lee Jr., M. W. Catalyst-Free Polyhydroboration of Dodecaborate Yields Highly Photoluminescent Ionic Polyarylated Clusters. *Angew. Chem. Int. Ed.* **2017**, *56*, 138-142. (b) Messina, M. S.; Axtell, J. C.; Wang, Y.; Chong, P.; Wixtrom, A. I.; Kirlikovali, K. O.; Upton, B. M.; Hunter, B. M.; Shafaat, O. S.; Khan, S. I.; Winkler, J. R.; Gray, H. B.; Alexandrova, A. N.; Maynard, H. D.; Spokoyny, A. M. Visible-Light-Induced Olefin Activation Using 3D Aromatic Boron-Rich Cluster Photooxidants. *J. Am. Chem. Soc.* **2016**, *138*, 6952-6955. (c) Kirlikovali, K. O.; Axtell, J. A.; Gonzalez, A.; Phung, A. C.; Khan, S. I.; Spokoyny, A. M. Luminescent Metal Complexes Featuring Photophysically Innocent Strong-Field Chelating Boron Cluster Ligands. *Chem. Sci.* **2016**, *7*, 5132-5138.

(13) Hawthorne, M. F.; Maderna, A. Applications of Radiolabeled Boron Clusters to the Diagnosis and Treatment of Cancer. *Chem. Rev.* **1999**, *99*, 3421-3434.

(14) Qian, E. A., Wixtrom, A. I.; Axtell, J. C.; Saebi, A.; Jung, D.; Rehak, P.; Han, Y.; Moully, E. H.; Mosallaei, D.; Chow, S.; Messina, M. S.; Wang, J. Y.; Royappa, A. T.; Rheingold, A. L.; Maynard, H. D.; Kral, P.; Spokoyny, A. M. Atomically precise organomimetic cluster nanomolecules assembled via perfluoroaryl-thiol S_NAr chemistry. *Nat. Chem.* **2017**, *9*, 333-340.

(15) Kim, K.-C.; Reed, C. A.; Elliot, D. W.; Mueller, L. J.; Tham, F.; Lin, L.; Lambert, J. B. Crystallographic Evidence for a Free Silylium Ion. *Science* **2002**, *297*, 825-827.

(16) Bolskar, R. D.; Mathur, R. S.; Reed, C. A. Synthesis and Isolation of a Fullerene Carbocation (C_{76}^+). *J. Am. Chem. Soc.* **1996**, *118*, 13093-13094.

(17) Xie, Z.; Bau, R.; Reed, C. A. A Crystalline $[H_9O_4]^+$ Hydronium Ion Salt with a Weakly Coordinating Anion. *Inorg. Chem.* **1995**, *34*, 5403-5404.

(18) Xie, Z.; Bau, R.; Reed, C. A. "Free" $[Fe(tpp)]^+$ Cation: A New Concept in the Search for the Least Coordinating Anion. *Angew. Chem. Int. Ed.* **1995**, *33*, 2433-2434.

(19) (a) Zhang, X.; Yan, H. Transition metal-induced B–H functionalization of *o*-carborane. *Coord. Chem. Rev.* **2017**, *378*, 466−482. (b) Cheng, R.; Qiu, Z.; Xie, Z. Iridium-catalysed regioselective borylation of carboranes via direct B–H activation. *Nat. Commun.* **2017**, *8*, 1482714833.

(20) (a) Zhang, X.; Zheng, H.; Li, J.; Xu, F.; Zhao, J.; Yan, H. Selective Catalytic B–H Arylation of o-Carboranyl Aldehydes by a Transient Directing Strategy. *J. Am. Chem. Soc.* **2017**, *139*, 14511−14517.

(b) Li, C.-X.; Zhang, H.-Y.; Wong, T.-Y.; Cao, H.-Ji.; Yan, H.; Lu, C.-S. Pyridyl-Directed Cp*Rh(III)-Catalyzed B(3)–H Acyloxylation of *o*-Carborane. *Org. Lett.* **2017**, *19*, 5178−5181.

(21) (a) Cao, K.; Huang, Y.; Yang, J.; Wu, J. Palladium catalyzed selective mono-arylation of *o*-carboranes via B–H activation. *Chem. Commun.* **2015**, *51*, 7257−7260. (b) Xu, T.-T.; Cao, K.; Wu, J.; Zhang, C.-Y.; Yang, J. Palladium-Catalyzed Selective Mono-/Tetraacetoxylation of *o*-Carboranes with Acetic Acid via Cross Dehydrogenative Coupling of Cage B−H/O−H Bonds. *Inorg. Chem.* **2018**, 57, 2925−2932.

(22) (a) Yu, W.-B.; Cui, P.−F.; Gao, W.-X.; Jin, G.-X. B−H activation of carboranes induced by late transition metals. *Coord. Chem. Rev.* **2017**, *350*, 300−319. (b) Duttwyler, S. Recent advances in B–H functionalization of icosahedral carboranes and boranes by transition metal catalysis. *Pure Appl. Chem.* **2018**, *90*, 733−744.

(23) Guennic, L.; Jiao, H.; Kahlal, S.; Saillard, J.-Y.; Halet, J.-F.; Ghosh, S.; Shang, M.; Beatty, A. M.; Rheingold, A. L.; Fehlner, T. P. Synthesis and Characterization of Hypoelectronic Rhenaboranes. Analysis of the Geometric and Electronic Structures of Species Following Neither Borane nor Metal Cluster Electron-Counting Paradigms. *J. Am. Chem. Soc.* **2004**, *126*, 3203-3217.

(24) (a) Bregadze, V. I. Dicarba-closo-dodecaboranes $C_2B_{10}H_{12}$ and their derivatives. *Chem. Rev.* **1992**, *92*, 209-223. (b) Morrison, J. A. Chemistry of the polyhedral boron halides and the diboron tetrahalides. *Chem. Rev.* **1991**, *91*, 35-48. (c) Knoth, W. H.; Miller, H. C.; Sauer, J. C.; Balthis, J. H.; Chia, Y. T.; Muetterties, E. L. Chemistry of Boranes. IX. Halogenation of $B_{10}H_{10}^{-2}$ and $B_{12}H_{12}^{-2}$. *Inorg. Chem.* **1964**, *3*, 159-167.

(25) (a) Dhayal, R. S.; Sahoo, S.; Ramkumar, V.; Ghosh, S. Substitution at Boron in Molybdaborane Frameworks: Synthesis and Characterization of Isomeric $(\eta^5\text{-}C_5Me_5Mo)_2B_5H_nX_m$ (when X = Cl: n = 5, 7, 8; m = 4, 2, 1 and X = Me: n = 6, 7; m = 3, 2). *J. Organomet. Chem.* **2009**, *694*, 237-243. (b) Geetharani, K.; Krishnamoorthy, B. S.; Kahlal, S.; Mobin, S. M.; Halet, J-F.; Ghosh, S. Synthesis and Characterization of Hypoelectronic Tantalaboranes. Comparison of the Geometric and Electronic Structures of $[(Cp^*TaX)_2B_5H_{11}]$ (X = Cl, Br and I). *Inorg. Chem.* **2012**, *51*, 10176-10184.

(26) (a) Sharmila, D.; Ramalakshmi, R.; Chakrahari, K. K. V.; Varghese, B.; Ghosh, S. Synthesis, characterization and crystal structure analysis of cobaltaborane and cobaltaheteroborane clusters. *Dalton Trans.* **2014**, *43*, 9976-9985. (b) Yuvaraj, K.; Roy, D. K.; Arivazhagan, C.; Mondal, B.; Ghosh, S. Chemistry of early and late transition metallaboranes: synthesis and structural characterization of periodinated dimolybdaborane $[(Cp^*Mo)_2B_4H_3I_5]$. *Pure Appl. Chem.* **2015**, *87*, 195-204.

(27) Prakash, R.; Bakthavachalam, K.; Varghese, B.; Ghosh S. Chlorination of the terminal hydrogen atoms in the hydrogen-rich group 5 dimetallaboranes $(Cp^*M)_2(B_2H_6)_2$ (M = Nb, Ta). *J. Organomet. Chem.* **2017**, *846*, 372-378.

(28) Bose, S. K.; Geetharani, K.; Ramkumar, V.; Mobin, S. M.; Ghosh, S. Fine Tuning of Metallaborane Geometries: Chemistry of Metallaboranes of Early Transition Metals Derived from Metal Halides and Monoborane Reagents. *Chem. Eur. J.* **2009**, *15*, 13483-13490.

(29) (a) Klumpp, E.; Marko, L.; Bor, G. Schwefelhaltige Metallcarbonyle, V. Reaktionen von Kobaltcarbonyl mit Schwefelwasserstoff, Mercaptanen und Disulfiden. *Chem. Ber.* **1964**, *97*, 926-933. (b) Klumpp, E.; Bor, G.; Marko, L. Schwefelhaltige Metallcarbonyle, VIII. Reaktionen von Dikobaltoctacarbonyl mit Thiophenol und Thiophenolderivaten. *Chem. Ber.* **1967**, *100*, 1451-1458.

(30) Schulenberg, N.; Ciobanu, O; Kaifer, E.; Wadepohl, Himmel, H.-J. The Doubly Base-Stabilized Diborane(4) $[HB(\mu\text{-hpp})]_2$(hpp = 1,3,4,6,7,8-hexahydro-2H-pyrimido[1,2-a]pyrimidinate): Synthesis by Catalytic Dehydrogenation and Reactions with S_8 and Disulfides. *Eur. J. Inorg. Chem.* **2010**, 5201–5210.

(31) Bose, S. K.; Geetharani, K.; Ramkumar, V.; Varghese, B.; Ghosh, S. Chemistry of Vanadaboranes: Synthesis, Structures, and Characterization of Organovanadium Sulfide Clusters with Disulfido Linkage. *Inorg. Chem.* **2010**, *49*, 2881–2888.

(32) (a) Wadepohl, H. Hypoelectronic Dimetallaboranes. *Angew. Chem. Int. Ed.* **2002**, *41*, 4220-4223. (b) Sahoo, S.; Reddy, K. H. K.; Dhayal, R. S.; Mobin, S. M.; Ramkumar, V.; Jemmis E. D.; Ghosh. S. Chlorinated Hypoelectronic Dimetallaborane Clusters: Synthesis, Characterization and Electronic Structures of $(\eta^5\text{-}C_5Me_5W)_2B_5H_nCl_m$ (n = 7, m = 2 and n = 8, m = 1). *Inorg. Chem.* **2009**, *48*, 6509-6516.

(33) Abernethy, C. D.; Bottomley, F.; Decken, A. Organometallic Halides: Preparation and Physical and Chemical Properties of Tris[(η-pentamethylcyclopentadienyl)dichlorovanadium], $[(\eta\text{-}C_5Me_5)V(\mu\text{-}Cl)_2]_3$. *Organometallics* **1997**, *16*, 1865-1869.

(34) Ryschkewitsch, G. E.; Nainan, K. C. Octahydrotriborate(1-) $[B_3H_8]$ salt. *Inorg. Synth.* **1974**, *15*, 113−114.

(35) (a) Led, J. J.; Gesmar, H. Application of the linear prediction-method to NMR-spectroscopy. *Chem. Rev.* **1991**, *91*, 1413−1426. (b) Yang, L.; Simionescu, R.; Lough, A.; Yan, H. Some observations relating to the stability of the BODIPY fluorophore under acidic and basic conditions. *Dyes Pigm.* **2011**, *91*, 264−267. (c) Weiss, R.; Grimes, R. N. Sources of Line Width in Boron-11 Nuclear Magnetic Resonance Spectra. Scalar Relaxation and Boron-Boron Coupling in B_4H_{10} and B_5H_9. *J. Am. Chem. Soc.* **1978**, *100*, 1401−1405.

(36) *APEX2*, *SAINT*, and *SADABS*; Bruker AXS Inc.: Madison, WI, 2004.

(37) (a)Sheldrick, G. M. *SHELXS-97*; University of Göttingen: Göttingen, Germany, 1997. (b) Sheldrick, G. M. Crystal structure refinement with SHELXL. *Acta Crystallogr., Sect. C: Struct. Chem.* **2015**, *C71*, 3−8.

(38) Dolomanov, O. V.; Bourhis, L. J.; Gildea, R. J.; Howard, J. A. K.; Puschmann, H. *J. Appl. Crystallogr.* **2009**, *42*, 339–341.

(39) Frisch, M. J.; et al. Gaussian 09; Gaussian, Inc.: Wallingford, CT, 2010.

(40) Schmider, H. L.; Becke, A. D. Optimized density functionals from the extended G2 test set. *J. Chem. Phys.* **1998**, *108*, 9624-9631.

(41) (a) Glendening, E. D.; Reed, A. E.; Carpenter, J. E.; Weinhold, F.; NBO Program 3.1, W. T. Madison, 1988; (b) Reed, A. E.; Curtiss, L. A.; Weinhold, F. Intermolecular interactions from a natural bond orbital, donor-acceptor viewpoint. *Chem. Rev.*, **1988**, *88*, 899–926. (c) Weinhold, F.; Landis, R. Valency and bonding: A natural bond orbital donor-acceptor perspective, Cambridge University Press, Cambridge, U.K., 2005.

(42) Lu, T.; Chen, F. Multiwfn: A multifunctional wavefunction analyser. *J. Comput. Chem.* **2012**, *33*, 580–592.

(43) GaussView, Version 3.09, Dennington II., Keith, R. T.; Millam, J.; Eppinnett, K.; Hovell, W. L.; Gilliland, R. Inc, Semichem, Shawnee Mission, KS, 2003.

(44) Zhurko, G. A. http://www.chemcraftprog.com.

.